U.S. DEPARTMENT OF COMMERCE
National Technical Information Service

PB-257 715

Detection of Atmospheric Pollutants at Parts-Per-Billion Levels by Infrared Spectroscopy

National Environmental Research Center, Research Triangle Park, N C

1973

272035

CLEARED FOR PUBLICATION

PB 257 715

DETECTION OF ATMOSPHERIC POLLUTANTS AT PARTS-PER-BILLON LEVELS BY INFRARED SPECTROSCOPY

by

Philip L. Hanst

Allen S. Lefohn

Bruce W. Gay, Jr.

Environmental Protection Agency
National Environmental Research Center
Research Triangle Park, North Carolina

REPRODUCED BY
NATIONAL TECHNICAL
INFORMATION SERVICE
U. S. DEPARTMENT OF COMMERCE
SPRINGFIELD, VA. 22161

BIBLIOGRAPHIC DATA SHEET	1. Report No.	2.	3. Recipient's Accession No. PB-257 715
4. Title and Subtitle Detection of Atmospheric Pollutants at Parts-Per-Billion Levels by Infrared Spectroscopy			5. Report Date 1973 6.
7. Author(s) Philip L. Hanst, Allen S. Lefohn, and Bruce W. Gay, Jr.			8. Performing Organization Rept. No.
9. Performing Organization Name and Address National Environmental Research Center, Research Triangle Park, N. C.			10. Project/Task/Work Unit No. 11. Contract/Grant No.
12. Sponsoring Organization Name and Address			13. Type of Report & Period Covered 14.

15. Supplementary Notes

16. Abstracts

Infrafed detection of air pollutants has been extended to the parts-per-billion sensitivity range. The increased detection sensitivity results from the use of the scanning Michelson interferometer, cooled solid state detectors, the fast mini-computer, and the multiple pass long path cell. Forming ratios of spectra with the aid of the computer extracts obscure information and minimizes the interferences of atmospheric water and carbon dioxide. Almost all of the significant gaseous pollutants can be measured by the method described, even at concentrations smaller than one part pollutant to one billion parts air.

17. Key Words and Document Analysis. 17a. Descriptors

*Infrared spectroscopy,
*Spectroscopic analysis,

Air pollution,
Interferometers,
Infrared detectors,
Water vapor,
Carbon dioxide,
Concentration(Composition),
Troposphere,
Lower atmosphere,
Micro analysis.

17b. Identifiers/Open-Ended Terms

*Air pollution detection.

17c. COSATI Field Group 7D

18. Availability Statement	19. Security Class (This Report)	21. No. of Pages
National Technical Information Service Springfield, Va. 22161	UNCLASSIFIED	52p
	20. Security Class (This Page) UNCLASSIFIED	22. Price 4.50/2.25

FORM NTIS-35 (REV. 10-73) ENDORSED BY ANSI AND UNESCO. THIS FORM MAY BE REPRODUCED USCOMM-DC 8265-P74

ABSTRACT

Infrared detection of air pollutants has been extended to the parts-per-billion sensitivity range. The increased detection sensitivity results from the use of the scanning Michelson interferometer, cooled solid state detectors, the fast mini-computer, and the multiple pass long path cell. Forming ratios of spectra with the aid of the computer extracts obscure information and minimizes the interferences of atmospheric water and carbon dioxide. Almost all of the significant gaseous pollutants can be measured by the method described, even at concentrations smaller than one part pollutant to one billion parts air.

I. Introduction

A. Infrared Spectroscopy in Air Pollution Research

Infrared spectroscopy has been applied to the study of the polluted atmosphere for many years. Some early work used the sun as the infrared source.[1,2] The solar spectrum gives the integrated total of pollutants along a slant path up through the polluted layer. If the sun is low, the path through the pollution is very long and small amounts of pollution can be seen. The interference by atmospheric water vapor and carbon dioxide is the principal limitation of solar observations. The early work was done with prism spectrometers of low resolution, which also limited the amount of information acquired. There have been many studies of the solar infrared spectrum with high resolution grating instruments, but generally these studies have been made through clean air. The basic reference work from such studies is the volume published by Migeotte, Neven and Swensson.[3]

The atmospheric infrared spectrum has been studied by ~~Gates~~ Murcray et al. over a single long path from a balloon-borne spectrometer aimed at the sun.[4] In that work, the long optical path was confined to the upper atmosphere, so that water vapor interference was largely eliminated. Distinctive nitric acid bands were among those observed.

For the study of the pollution in the lower troposphere, a long enclosed folded path is better than a single path up to the sun. There are several advantages. First, the length of folded path can be adjusted to optimize detection in the various regions of the infrared spectrum. Second, the path does not pass through any excess unpolluted air which would contribute water and CO_2 absorption. Third, the air pressure in the vessel can be reduced,

thus enhancing the detectability of certain pollutants and decreasing the interferences.

Infrared studies of pollutants over a 200 meter folded path were carried out in 1954 in the laboratory of the Franklin Institute and later continued in the field.[5,6] During a period of several years, many basic facts on the photochemistry of air pollution were brought to light in these studies.

Among the results were the discovery and identification of the peroxy acyl nitrates (PAN's) and the spectroscopic proof of ozone formation in the Los Angeles air. A similar long path cell and spectrometer system has been in use at the General Motors Laboratories for many years and has likwise led to a number of important papers on the photochemistry of air pollution.[7,8]

Although the long path infrared method has had much success in pollution measurement, the full potential of the method has not yet been reached. Applications of infrared methods to atmospheric studies have been slow in responding to the many new developments of optical science during the past ten years. Instrumentation used in the work reported here brings several new devices to bear on the pollution problem and extends the infrared method to a range of pollutant concentrations about one hundred times lower than has been previously reached.

The infrared method is based on the distinctive nature of the absorption bands in the vibration-rotation spectrum. Every hetero-nuclear diatomic molecule and every polyatomic molecule has at least one characteristic infrared band. Only homonuclear diatomic molecules and monatomic gases do

not. Almost all gaseous pollutants can therefore be seen in the infrared.

The spectrum of a given molecular species differs from all other spectra. These differences are most distinctive in the case of the smaller molecules which have fine detail in their infrared bands at atmospheric pressure. High resolution instruments use this fine structure to detect a pollutant in the presence of other pollutants even if the infrared bands overlap. High resolution instruments also distinguish the pollutant absorption from the water vapor absorption which occurs throughout the spectrum.

Pollutants of high molecular weight have smooth infrared bands without fine structure at atmospheric pressure. When these overlap they are difficult to separate. Reducing sample pressure brings fine structure into such bands and does allow separation. However, a mixture of high molecular weight pollutants such as a gasoline vapor is more easily measured by gas chromatography than by infrared spectroscopy.

The principal limitation on infrared detection of pollutants is the interference by atmospheric water vapor. Water lines are everywhere in the spectrum because there is so much water in the air. Drying an air sample before analysis is to be avoided because in removing the water one runs the risk of altering the concentrations of pollutants to be measured. The infra-ed technique must be designed to work in the presence of the water lines. Ways of avoiding interferences in the spectrum have been discussed in a recent review article[9] and will be discussed further in the present paper.

B. Ways to Improve Detection Sensitivity

The detection sensitivity of an absorption experiment depends on: (1) the strength of the pollutant bands, (2) the noise in the spectral background, (3) the structural detail in the pollutant bands, and (4) the strength and structure of the bands of interfering gases. These factors are influenced by the instrumentation design and the operating technique.

Since the air pollutants are extremely low in concentration, their infrared absorption is extremely weak over short paths. When the spectrum is measured in transmitted light, the absorption signal is increased in proportion to the path length. Long paths, therefore, are almost universally used in air pollution spectroscopy.

Until recently the long path method was the only practical method of bringing out weak bands. Scanning lasers now give promise of providing a new technique in which one monitors the absorption per unit volume rather than the transmission. In this method the signal is increased by raising the power of the source while holding the path length constant. This new technique is still only in a rudimentary stage of development; and for the measurement of trace gases, the transmission mode of observing the spectrum is still far superior. By means of folded path cells, the present studies were carried out at path lengths of up to 720 meters.

Fluctuations in detector output create noise in the spectral background. Detectivity, the figure of merit of detector performance, must be as high as practical, which is to say that the electromagnetic wave must generate a

large detectable signal but only a small amount of noise. Detector research in the past two decades has steadily increased the available detectivities. Furthermore, detector response times have been shortened, spectral ranges have been widened, and cooling systems have been much improved. Thus, there is much to be gained in a pollution detection system by using the most up-to-date detectors.

System performance is further optimized by using instruments which conserve the available energy and examine the spectrum in an efficient manner. This depends on the instrumental properties of throughput and multiplexing. Throughput is the property of conserving energy while processing the spectrum. A conventional type of grating spectrometer has low throughput because the narrow entrance slit passes only a portion of the incident light; and furthermore, there are reflection losses at the grating, mirrors, choppers, and other components. In contrast, non-dispersive instruments generally have high throughput.

Multiplexing is the simultaneous observation of multiple spectral resolution elements. At a fixed resolution, multiplexing permits faster data acquisition. A photographic spectrograph is a multiplexing instrument but a scanning monochromator is not. Non-dispersive analyzers generally have a high degree of multiplexing. In Michelson interferometers, the signal-to-noise gain resulting from multiplexing is equal to the square root of the number of resolution elements simultaneously observed. This can be a factor of one hundred or more. Other types of multiplexing instruments can have even higher gain factors.[9]

High spectral resolution is also essential to high detection sensitivity because it increases the information content of the spectrum. A high degree of spectral information allows one to separate pollutant bands and to make accurate quantitative measurements.

C. Ways to Reduce Interferences

If there is spectral fine structure in the bands being observed, interferences can be reduced by using high spectral resolution. Lines which appear to overlap under low resolution will be separated as resolution is increased. If there is no spectral fine structure, there is nothing to be gained by increasing the resolution. This is the case for many of the larger pollutant molecules at atmospheric pressure.

In almost all cases, fine structure can be introduced into the spectrum by reducing the sample pressure. Of course, reducing the pressure may sacrifice some detection sensitivity because it removes pollutant from the light path. The optimum point in the trade-off between sensitivity and selectivity will be determined by the complexity of the spectral region under study.

Interferences are also removed by processing the spectrum in various ways. For many years the double-beam ratio-recording technique has been the principal method of reducing interferences. There are two ratio recording methods: optical and computational. Up to the present time the optical method has been widely used. Two long path cells are used simultaneously. A clean air sample is placed in the reference cell, and the contaminated air sample is placed in the sample cell. The instrument then scans the spectrum while looking through both cells and recording

the ratio of the transmissivities. The interfering bands--such as the atmospheric water bands--cancel out, leaving only the pollutant bands.

The computational ratio recording technique has only recently been made possible through the development of the Michelson interferometer-spectrometer.[10] Here, only a single long path cell is required; and the two spectra are recorded successively. Each spectrum is extracted from its interferogram and stored in a computer in digital form. Ratios, differences, or other functions can be plotted at all points in the two spectra. These techniques of processing the spectra will be illustrated in the following sections.

II. Instrumentation and Technique

A. The Optical System

The optical components of the instrument system are diagrammed in Figure 1. The light from the Nerst glower, S, is projected by the spherical mirror, into the scanning interferometer. The beam is divided by the beam splitter, B, into two beams, one going to the scanning mirror, M_2, and the other to the fixed mirror, M_3. The mirror scan places a sine-wave modulation on each optical frequency in the recombined beam which passes out of the interferometer. These modulations have frequencies in the kilocycle (or audio frequency) range. The superposition of these waves constitutes the interferogram which is to be transformed in the computer to the infrared spectrum. This modulated infrared light passes into the multiple-pass cell and then into the detection system. A three mirror cell has been used, as described by White.[11] The eight-mirror cell described by Hanst offers greater optical throughput for this application

Figure 1. Optical Components

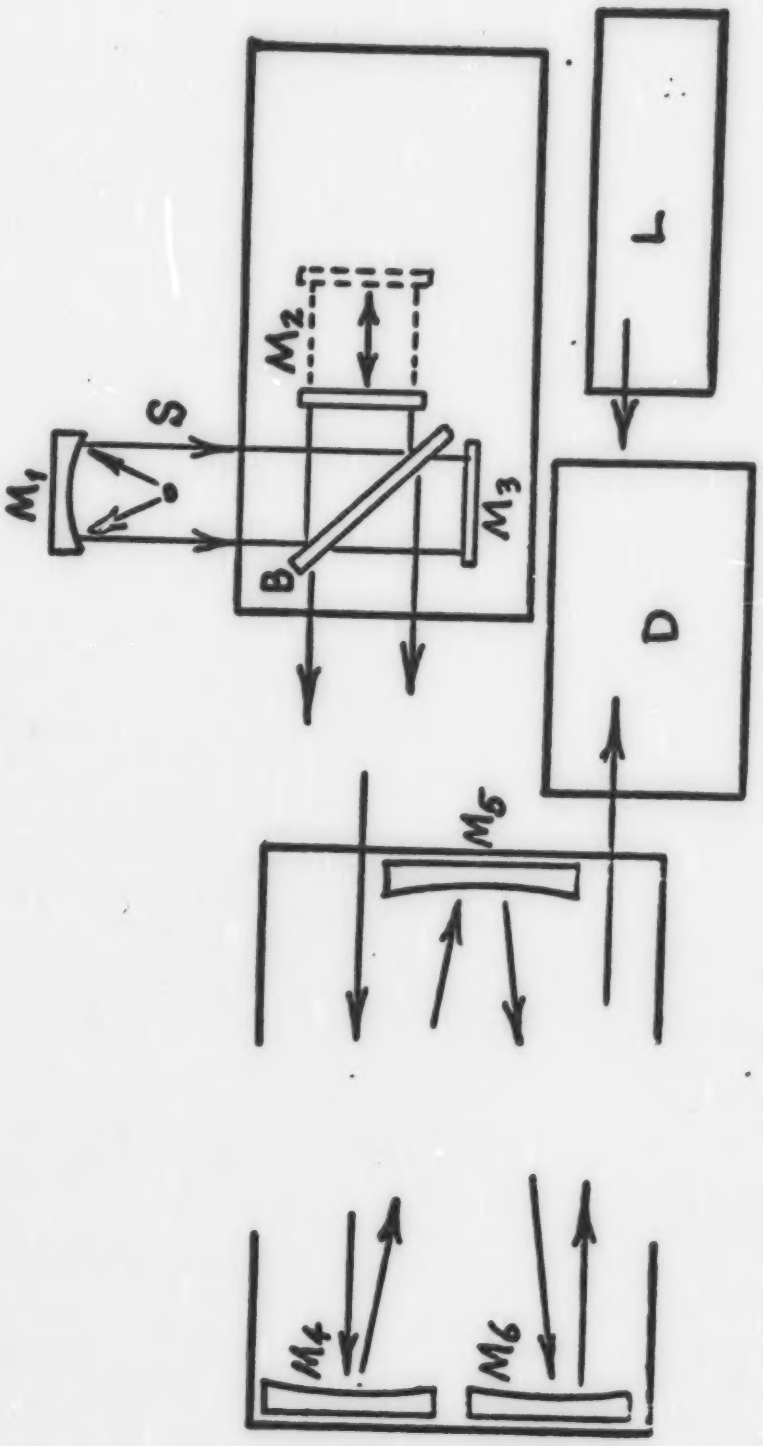
L
M2
S
M1
M3
B
D
M5
M4
M6

and will be used in the future.[9] In the three mirror cell a much enlarged image of the source is formed in the entrance aperture. From there the diverging light beam passes to the first of two mirrors at the far end, which it fills with little overlap. The collected light is returned to the mirror at the near end which reflects it to the second mirror at the far end. That mirror can then send the beam on its fourth pass either out to the detection system or through additional sets of four passes and then to the detection system.

Two sizes of multiple-pass cells have been used. Both are three mirror cells with spherical mirrors. The smaller of the two has a 2.25 meter base path. It can be used at path lengths over 200 meters (92 passes); but to date, it has been used mainly at 81 meters (36 passes). The base path of the larger cell is 8.7 meters. It has been used at total paths of 700 meters (80 passes). The mirrors for each cell were cut from two telescope mirrors. One was cut in half to form the two D-shaped mirrors at the out-of-focus end of the cell; the other was converted to a mushroom shape by two cutouts for the entrance and exit beams. The mirrors are mounted on lucite stands which clamp inside a pyrex pipe. The air inlet, the vacuum pump connection, and the potassium bromide entrance and exit windows are mounted on the lucite end plates of the cell.

A helium-neon laser, L, is used in the alignment and adjustment of the multiple-pass cells. The laser is a valuable adjunct to the system because its beam is so easily seen. The system is lined up in reverse with laser light and then the laser is replaced by the detection system.

The above description generally applies to both cells, but the larger cell is also equipped with ultraviolet lights for the study of photochemical reactions. The photochemical system will be described in detail in a later article.

No transfer optics are used between the multiple pass cells and the interferometer. Since the cells are long and narrow, the divergence angle of the transmitted light is small--about 2 degrees in the smaller cell and 1.5 degrees in the larger cell. These divergences are not much greater than the acceptance angle of the interferometer. It was found experimentally that attempts to collimate the light between the long path cell and the interferometer gave little signal gain.

An important aspect of the optical configuration is that the light source is at the input to the interferometer and the detector is at the output of the long path cell. This arrangement modulates the source light but does not modulate thermal emission which originates in the optical system. Thus the only radiation which is detected is that which has passed through the long path cell. There is no problem with background radiation, even at extremely long optical paths.

The interferometer is the Digilab Model 496. Its features include a germanium coated potassium bromide beam splitter, and an air supported scanning mirror with a four centimeter travel. A built-in reference interferometer controls and monitors the main mirror movement by means of the interference fringes of a helium-neon laser beam. Also included in the reference interferometer is a white light whose sharply peaked interferogram triggers the sampling of the main infrared interferogram.

Maximum obtainable resolution is 0.125 cm^{-1}. Wavelength precision is at least 0.1 cm^{-1} and probably much better than that. A photoconductive mercury-cadmium-telluride detector is used at liquid nitrogen temperature for work in the spectral region 600 cm^{-1} to 2300 cm^{-1}. Photovoltaic indium antimonide is used in the region 2000 cm^{-1} to 3950 cm^{-1}. This is cooled by liquid nitrogen. Interference filters are used to suppress noise and spectral overlaps, thus optimizing detection in selected spectral regions.

B. Data Processing and Computation

Data are processed by the Digilab Fourier Transform Spectrometer data system. The system consists of a 15-bit analog-to-digital converter, a NOVA 1200 mini computer of 4096 word capacity, a 131,000 word disk memory for data and programs, a teletypewriter for user control, and a digital plotter. There is also a magnetic tape storage system with a capacity for many hundreds of high resolution spectra. The relationship of the system components is diagrammed in Figure 2.

During a scan of the interferometer mirror, the detector signal is digitized at the number of points required for the desired spectral resolution and is stored in the computer. A chosen number of successive scans are added together in the computer, thus averaging the noise but building up the signal, the signal-to-noise ratio being increased by the square root of the number of scans. The single digitized sum interferogram is then transformed by the computer to a spectrum. This can immediately be plotted or it can be stored in the computer for further manipulation and future reference. The ability to manipulate the spectra is an outstanding feature of the spectrometer system. Through the teletypewriter commands

Figure 2. Fourier Transform Spectrometer Data System

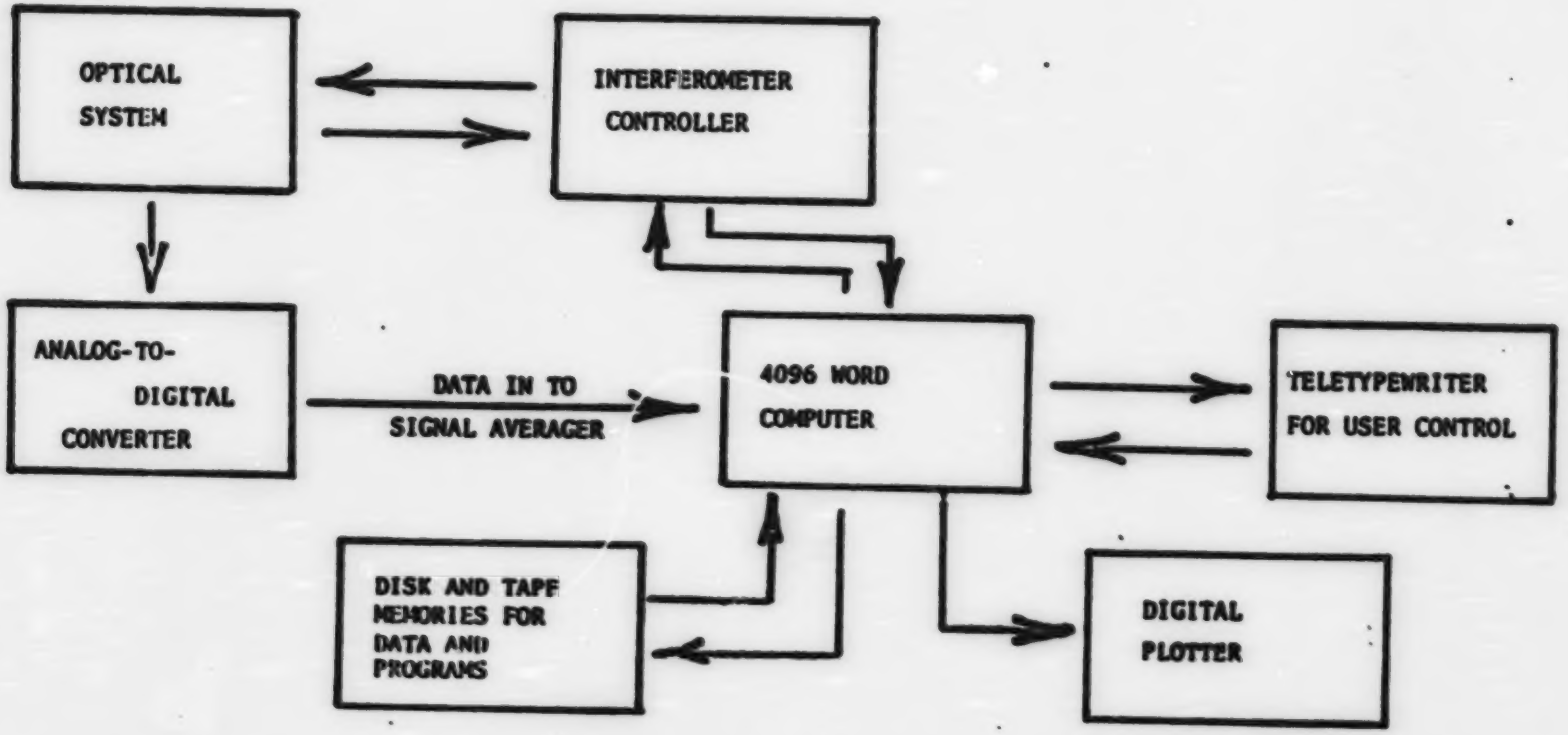
OPTICAL SYSTEM
INTERFEROMETER CONTROLLER
ANALOG-TO-DIGITAL CONVERTER
DATA IN TO SIGNAL AVERAGER
4096 WORD COMPUTER
TELETYPEWRITER FOR USER CONTROL
DISK AND TAPE MEMORIES FOR DATA AND PROGRAMS
DIGITAL PLOTTER

12a

the spectra are stored, retrieved, divided into each other, subtracted from each other, and plotted in various modes.

C. Reference Spectra for Ratio Recording

The atmospheric spectra recorded with the above described instruments have a very high information content as a result of the long path, the high spectral resolution, the high throughput and multiplexing of the interferometer, and the high sensitivity of the detectors. When these spectra are plotted out, however, the information may still be obscure because of the interferences. The spectra must therefore be manipulated in various ways to eliminate the interferences. These manipulations can result in great gains in pollutant detectability.

The principal way of removing interfering lines is to plot the ratio of the sample spectrum to a reference spectrum. Reference samples have been prepared from pollution-free tank air obtained from Scott Research Laboratories. The water vapor content of the reference air is adjusted by mixing air samples which have been placed in two plastic bags--one wet and one dry. The proportions of wet and dry air will give the humidity required.

When very weak pollutant lines are being sought, an exact balance of the water lines is required between the sample spectrum and the reference spectrum. This requires exact proportions of wet and dry reference air, which are not easy to create. The final adjustments in line strength are therefore made in the computer. A spectrum with too little water and one with too much water may be added in the computer with appropriate weighting factors to give the desired reference spectrum.

When searching for atmospheric impurities on such low levels as parts-per-billion, the purity of the reference air becomes an important consideration. Actually, long path infrared analysis is probably the best possible way of determining the impurity levels in the reference gases. When plotting a ratio spectrum, impurities in the reference gas which are not present in the air will show their spectra upside-down, which is to say that the lines will go above unity in the ratio plot. When the impurities also occur in the atmosphere, the spectra may be upside-down or right-side-up, depending on the relative concentrations. We have found great variations in the amount of impurities in tank gases. Some tank oxygen has contained several parts-per-million of methane which invalidated the measurement of atmospheric methane. Matheson zero-air may contain more carbon monoxide than the clean atmosphere. In 1971, Scott air contained the full atmospheric amount of CO_2 and about one-third the atmospheric amount of N_2O. In 1972, the Scott air was nearly free from CO_2 and N_2O. When the infrared spectrum of dry reference air is recorded in ratio mode over the spectrum of the evacuated absorption cell, impurities can be measured down to parts-per-billion concentration levels.

III. Resolution Considerations

The first set of three spectra, Figure 3, shows the gain in information content as resolution is increased. These are single beam plots of the spectrum of room air at atmospheric pressure with a path length of 432 meters. The region between 2000 cm^{-1} and 2300 cm^{-1} is shown at three different instrumental resolving powers. The upper spectrum recorded with 4 cm^{-1} resolution is similar in detail to spectra from prism instruments. The gross features of water and CO_2 absorption are evident, but much detail is lost. Increasing the resolution to 2 cm^{-1}, as in the middle spectrum, converts many of the single lines to multiplets. This happens when the multiplet splitting is approximately the same as the resolving power of the instrument. Some structure due to CO can be seen in the middle spectrum, but structure due to CO_2 cannot be seen. The bottom spectrum, at 1 cm^{-1} resolution, shows the CO more distinctly and also has clearly resolved the isotopic $^{13}C\,^{16}O_2$ lines between 2220 cm^{-1} and 2290 cm^{-1}. N_2O lines in the vicinity of 2205 cm^{-1} are still not resolved.

The instrument system is capable of a further 8-fold gain in resolution down to the limit of 0.125 cm^{-1}, and the fine structure of the air spectrum in the region 2150 cm^{-1} to 2300 cm^{-1} is shown in Figure 4 for this highest obtainable resolution. In this spectrum the families of lines from H_2O, CO, N_2O, and $^{13}C\,^{16}O_2$ are all clearly resolved. The water vapor concentration in the air sample was probably between 10,000 and 20,000 parts per million, which is to say that the water lines shown are in fact very weak lines. The CO concentration was probably between 0.1 and 0.2 parts per million, the lines

Figure 3. Increase of Spectral Information Content with Increasing Resolution. One atmosphere of room air at a path of 432 meters; resolving powers: top 4 cm^{-1}; center, 2 cm^{-1}; bottom, 1 cm^{-1}

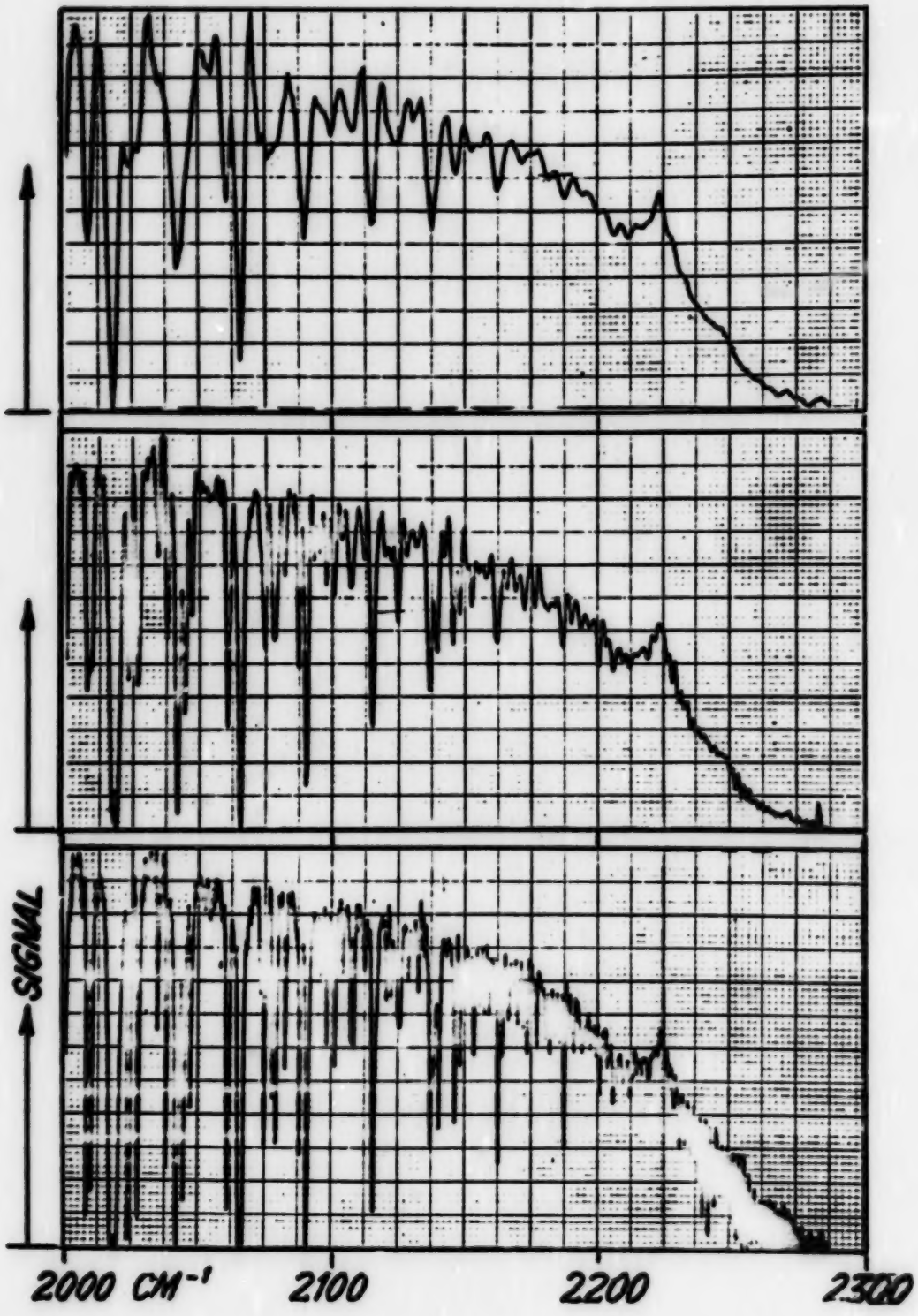
SIGNAL
2000 CM⁻¹
2100
2200
2300

Figure 4. A portion of the Atmospheric Spectrum at a resolving power of 0.125 cm^{-1}; one atmosphere of room air; path 432 meters

16a

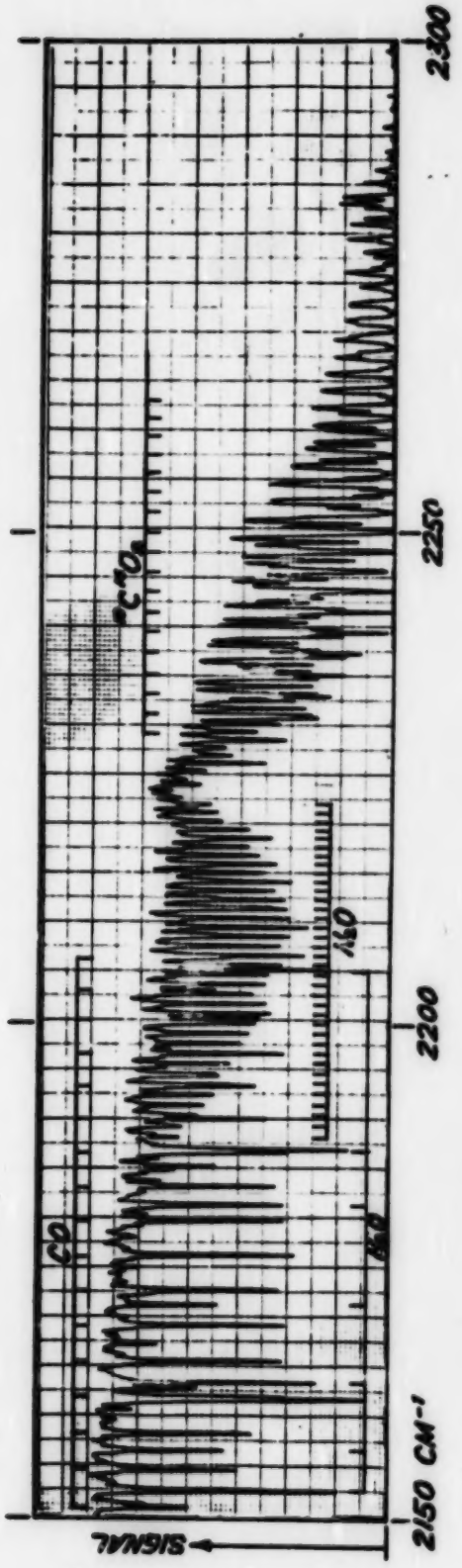

shown being among the strongest lines of the fundamental infrared band of the molecule. The N_2O concentration was the normal value, recently reported to be 0.25 parts per million.[12] The $^{13}C^{16}O_2$ concentration was approximately 3.2 parts per million, 1% of the total natural CO_2 concentration.

IV. Pressure Reduction Advantages

Figure 5 illustrates the increase in spectral fine structure of a polyatomic molecule which can result from a reduction of total pressure. There are two cases illustrated--ethane, which significantly increases its fine structure when total pressure is reduced from 760 Torr to 10 Torr, and propane, which does not increase its fine structure under the same pressure reduction. All four spectra were plotted with the spectrometer system set for resolution of 0.125 cm^{-1}. This comparison illustrates the point that for the heavier and more complex pollutant molecules there are so many spectral lines packed so closely together that extremely low pressure is required to separate individual lines.

A further advantage of pressure reduction is increased transmission in regions of water vapor interference. This advantage derives from the effects of pressure on the breadth of the absorption lines. Absorption is shifted out of the wings of the water lines in proportion to the reduction of pressure. At the same time the absorption coefficients at the centers of the water lines are increased by the reduction of pressure. However, the amount of energy absorbed near the line centers cannot increase because even at atmospheric pressure the line centers are totally absorbing. As pressure is reduced, the water not only changes its absorption line shape, but the amount

Figure 5. Effect of Total Pressure on the Fine Structure in the Infrared Bands of Ethane and Propane

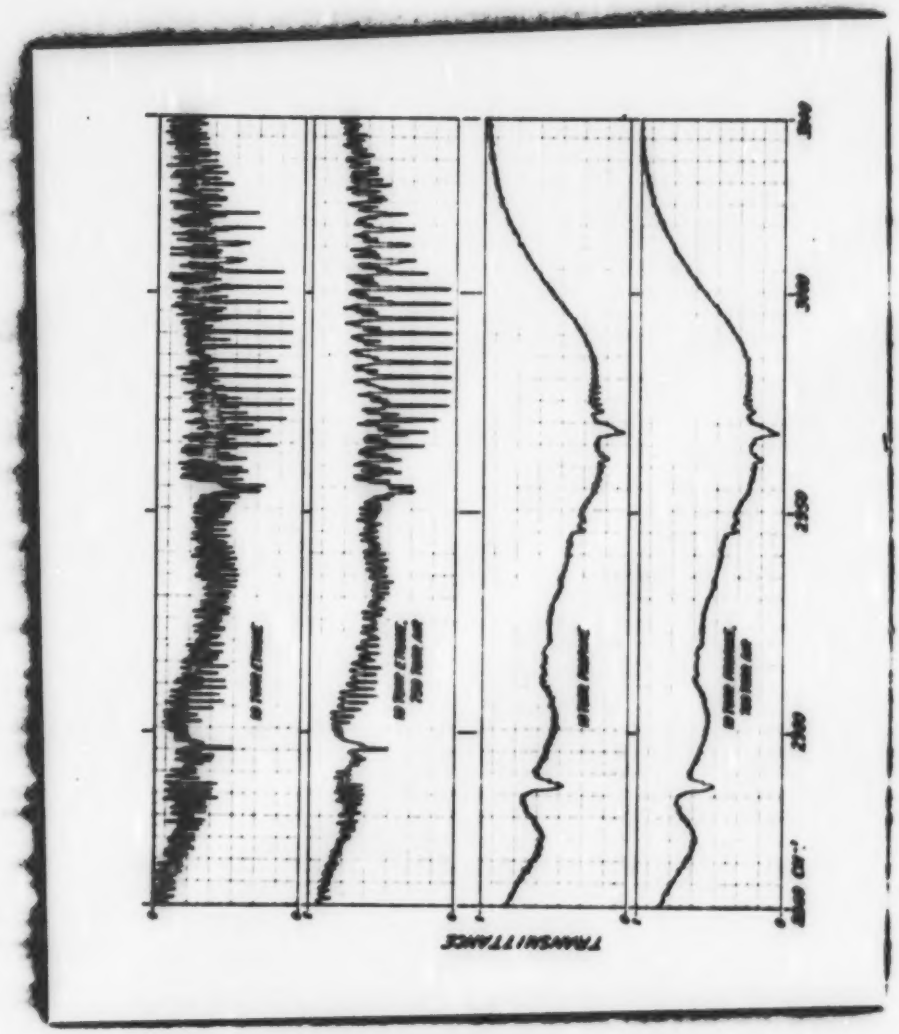
TRANSMITTANCE
3000
2500
2000
1500 cm⁻¹

of water in the light path is reduced. The net result is an increase in transmission of the water region almost in proportion to the inverse square of pressure. The pollutant absorption is also reduced as the pollutant molecules are removed from the light path, but only in direct proportion to the lowering of pressure. The net result is an increase in pollutant detectability. The choice of best operating pressure depends on the path length, the spectral region, the resolution, and the level of contaminants.

V. Ratio Recording

Figure 6 illustrates the advantage of ratio recording. The 2000 cm^{-1} to 2300 cm^{-1} region is again shown for clean air at 1 cm^{-1} resolution, but this time with a path of only 81 meters. This spectrum was recorded with the instrument system in a mobile van at Denver, Colorado, in October 1971. The upper spectrum is a single beam plot of the outside air at the Denver atmospheric pressure of 630 Torr while the spectrum just below it is a single beam plot of reference air. The third spectrum is the ratio plot of the first spectrum over the second. The reference air contains the normal 320 parts per million of CO_2 plus the added water, but it contains very little carbon monoxide and only about one-third the normal amount of nitrous oxide. There was actually a slight excess of reference air in the absorption cell so that water and CO_2 lines were overcompensated. This caused the ratio to go above unity for H_2O and CO_2, while it goes below for the CO and N_2O in the outside air sample. The water unbalance causes the weak water line at 2140 cm^{-1} to just compensate the absorption due to the CO line at the same frequency so that the CO line appears to be missing from the spectrum.

Figure 6. Illustration of the Advantages of Ratio Recording. Air at 630 Torr Pressure, Path 81 Meters

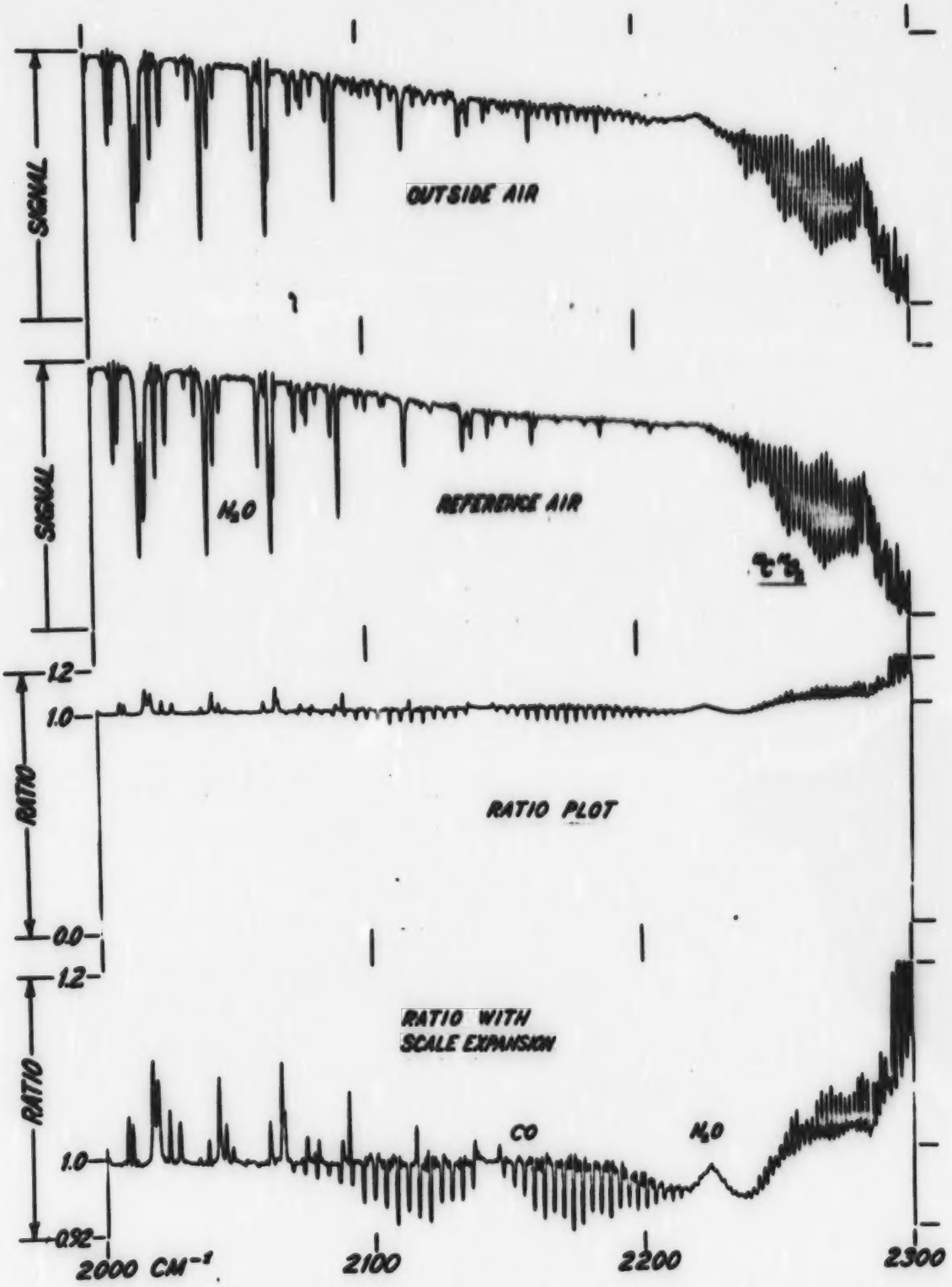
SIGNAL
OUTSIDE AIR
SIGNAL
H_2O
REFERENCE AIR
$C^{12}O_2$
1.2
1.0
RATIO
RATIO PLOT
0.0
1.2
RATIO WITH
SCALE EXPANSION
RATIO
CO
H_2O
1.0
0.92
2000 CM^{-1}
2100
2200
2300

The bottom spectrum of Figure 6 is a scale expanded plot of the ratio spectrum just above it. Since the signal-to-noise ratio was high, the scale expansion has made the absorption lines more obvious and easier to measure without bringing out background noise.

A ratio plot with a nearly exact balance of water absorption is shown in Figure 7, which covers the region of the strongest water vapor interference. Again, the path was 81 meters and the resolution 1 cm^{-1}; but in this case, the pressures were only 150 Torr. About 5 parts per million of NO_2 and ten parts per million of NO were added to the sample to produce the spectra. This figure illustrates how the spectrum "opens up" at lower pressures so that absorption bands can be seen between the water lines.

A difficulty of ratio plotting is illustrated by the several extraneous pen lines in the ratio plot of Figure 7. It can be seen that these erratic pen excursions take place at the center of the water lines. The reason is that there is practically no transmitted energy at the line centers in either the sample spectrum or the reference spectrum. The instrument takes the ratio of noise over noise, which may fall at random somewhere between zero and a very large number. This noise-over-noise problem becomes more serious as resolution is increased, and in the early stages of this investigation, the plotting of noise appeared to be the principal limitation of the technique. In response to this difficulty, the Digilab plotting program has now been altered to avoid the noise. In ratio plotting the computer now passes over those points in the spectrum where the energy level in the reference beam approaches the noise level in the spectrum. The improvement is reflected in the relatively clean ratio plot of Figure 8.

Figure 7. Ratio Plot in Region of Heaviest Water Vapor Interference. Air Pressure 150 Torr, Path 81 Meters; NO_2 Concentration About 5 PPM; NO Concentration About 10 PPM

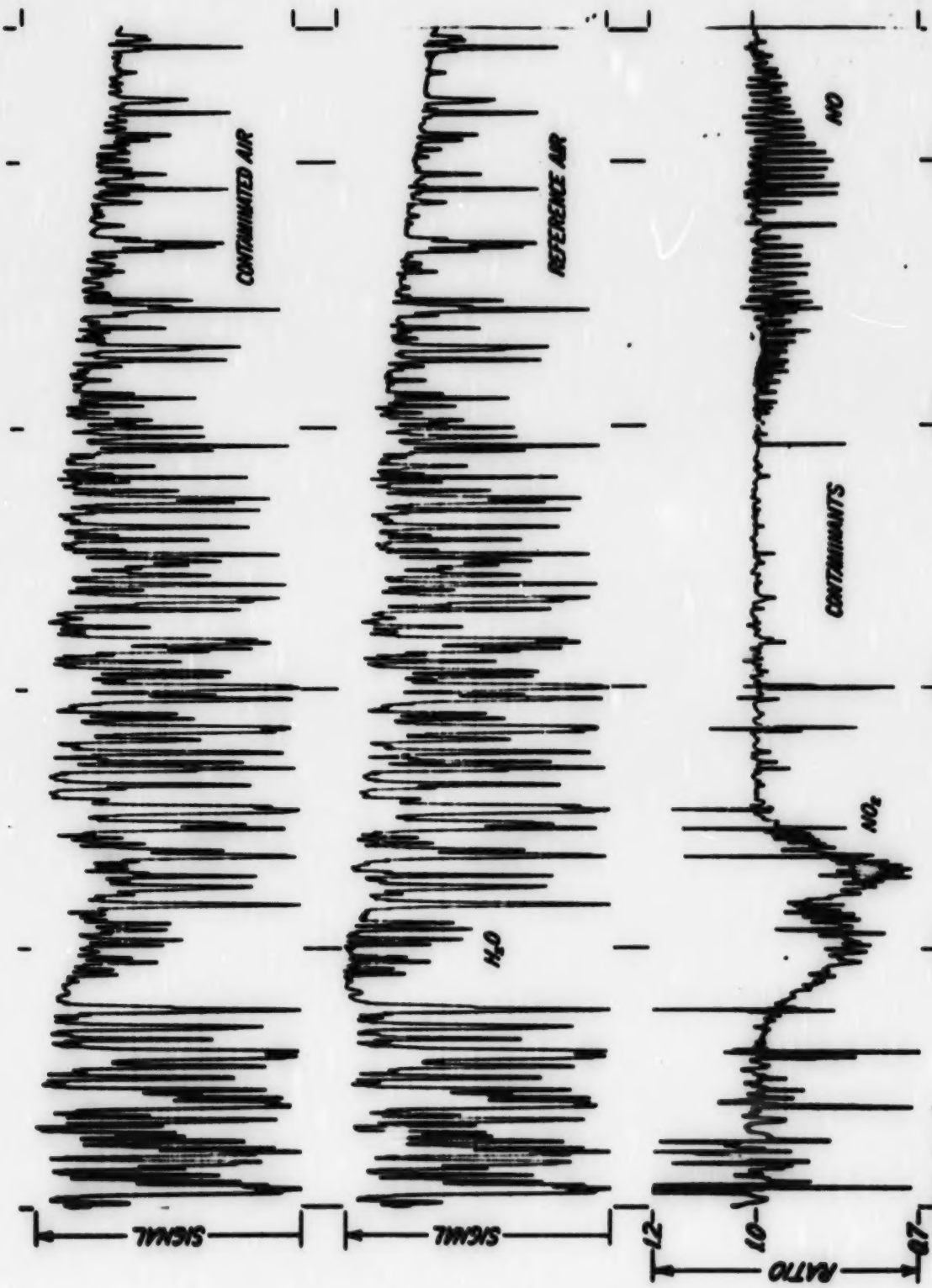
CONTAMINATED AIR
REFERENCE AIR
NO
CONTAMINANTS
H_2O
NO_2
SIGNAL
SIGNAL
RATIO
1900
1800
1700
1600
1500 CM⁻¹
1.2
1.0
0.7

VI. Atmospheric Spectra in the Region 700 cm^{-1} to 1400 cm^{-1}

As a further example of the performance of the system in air analysis, Figure 8 shows the atmospheric spectrum in the region 700 cm^{-1} to 1400 cm^{-1}. The path length was 418 meters through one atmosphere of air which was about half room air and half outside air collected on the highway. At the bottom is a single beam plot of the air spectrum showing mainly the prominent water and CO_2 lines. The upper spectrum is a smoothed, scale-expanded, ratio plot of the air spectrum over the spectrum of a mixture of tank air, H_2O and CO_2. The H_2O and CO_2 concentrations were adjusted to give cancellation of the interfering lines leaving only the pollutant lines shown. From references cited in Table I the concentrations of pollutants were calculated to be ethylene, 0.19 parts per million (PPM); acetylene, 0.25 PPM; propylene, 0.12 PPM; and formic acid, 0.16 PPM. The methane concentration was not calculated because of methane impurity in the reference air.

Figure 9 shows the measurement of 3 parts-per-hundred-million of ozone in outside air, recorded with a path length of 81 meters. This spectrum was recorded with the instrument system in the mobile van at Denver, Colorado. This ozone content can be considered typical of clean air on a sunny day. The ratio recorded spectrum in the figure shows a noise level approximately one thousandth as great as the total ratio signal.

Figure 10 shows the measurement of approximately 3 parts-per-hundred-million of nitric acid in room air with a path length of 471 meters. At the top is the sample spectrum; in the center is the reference spectrum, and on the bottom is the ratio spectrum. This spectrum was recorded at a resolution of 2 cm^{-1} and was plotted without smoothing to preserve the HNO_3

Figure 8. An Atmospheric Spectrum in the Region 700 cm^{-1} to 1400 cm^{-1}

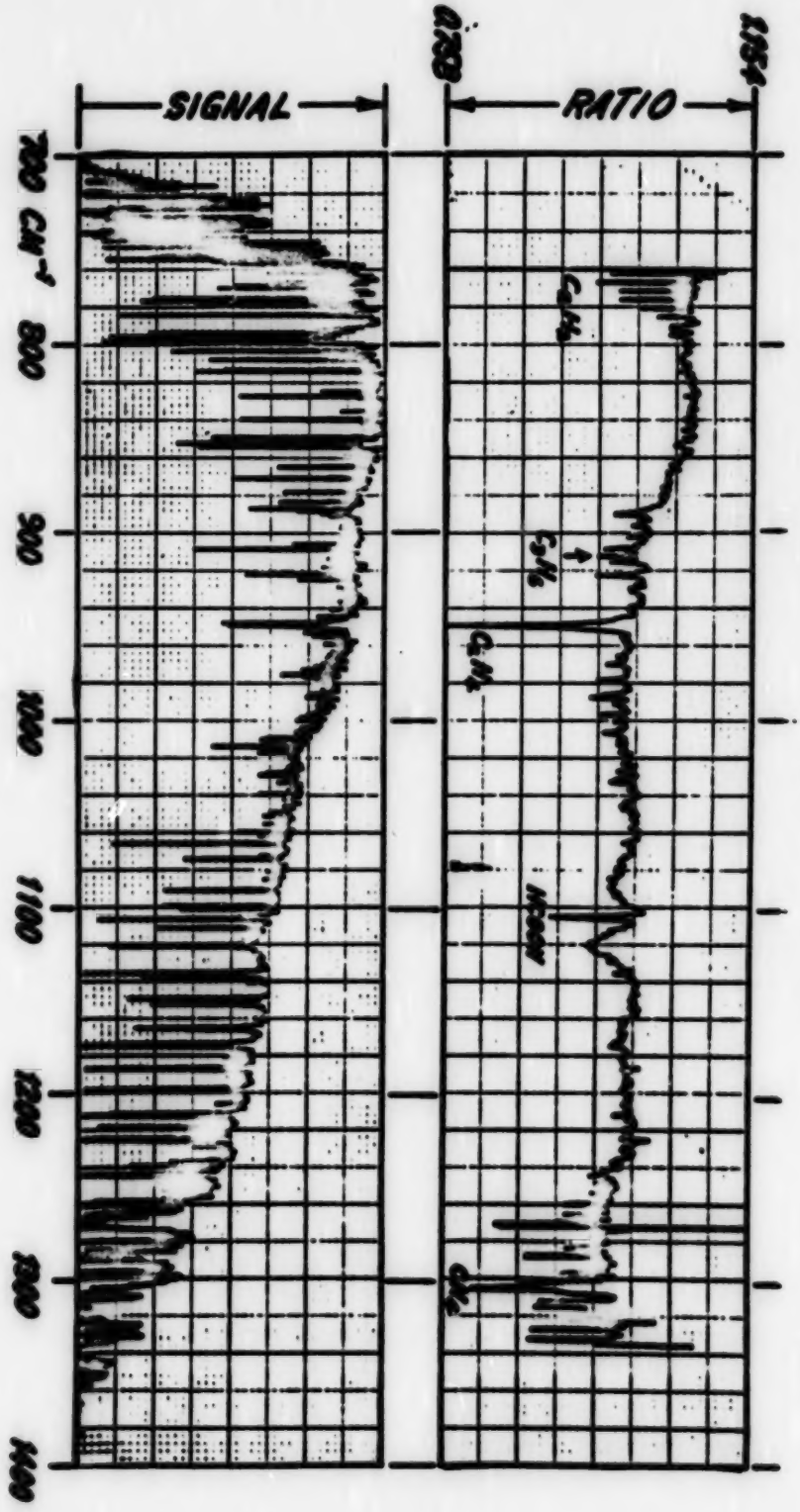
SIGNAL
RATIO
700 CM⁻¹
800
900
1000
1100
1200
1300
1400
1600
1515
1550
C-H
C-H
amide

Figure 9. Measurement of 3 PPHM O_3 in Outside Air. Path, 81 Meters; Resolution, 8 cm^{-1}

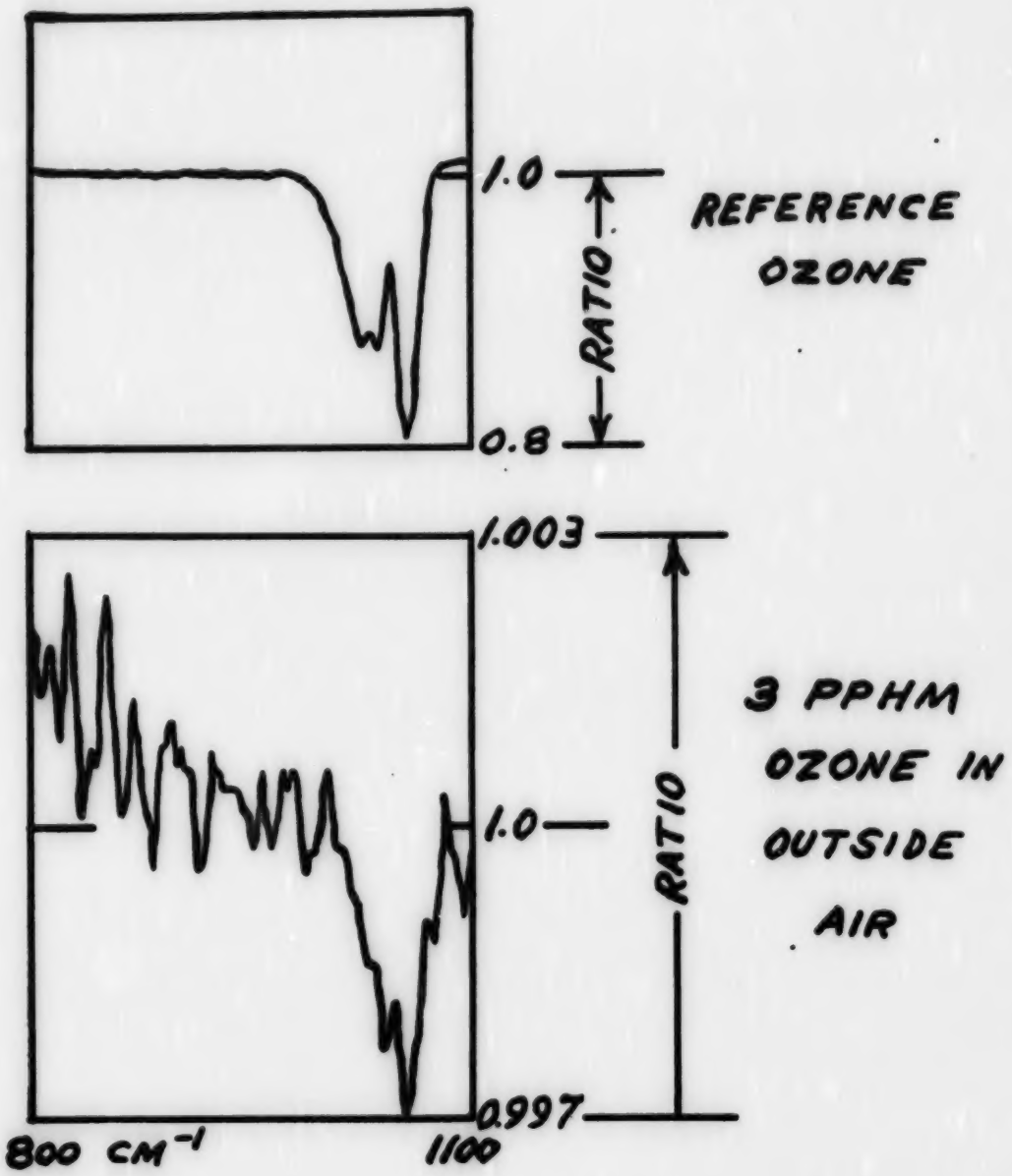
1.0
0.8
RATIO
REFERENCE
OZONE
1.003
1.0
0.997
RATIO
3 PPHM
OZONE IN
OUTSIDE
AIR
800 CM⁻¹
1100

Figure 10. Measurement of 3 PPHM HNO_3 in Room Air With a Path Length of 471 Meters; Resolution, 2 cm^{-1}

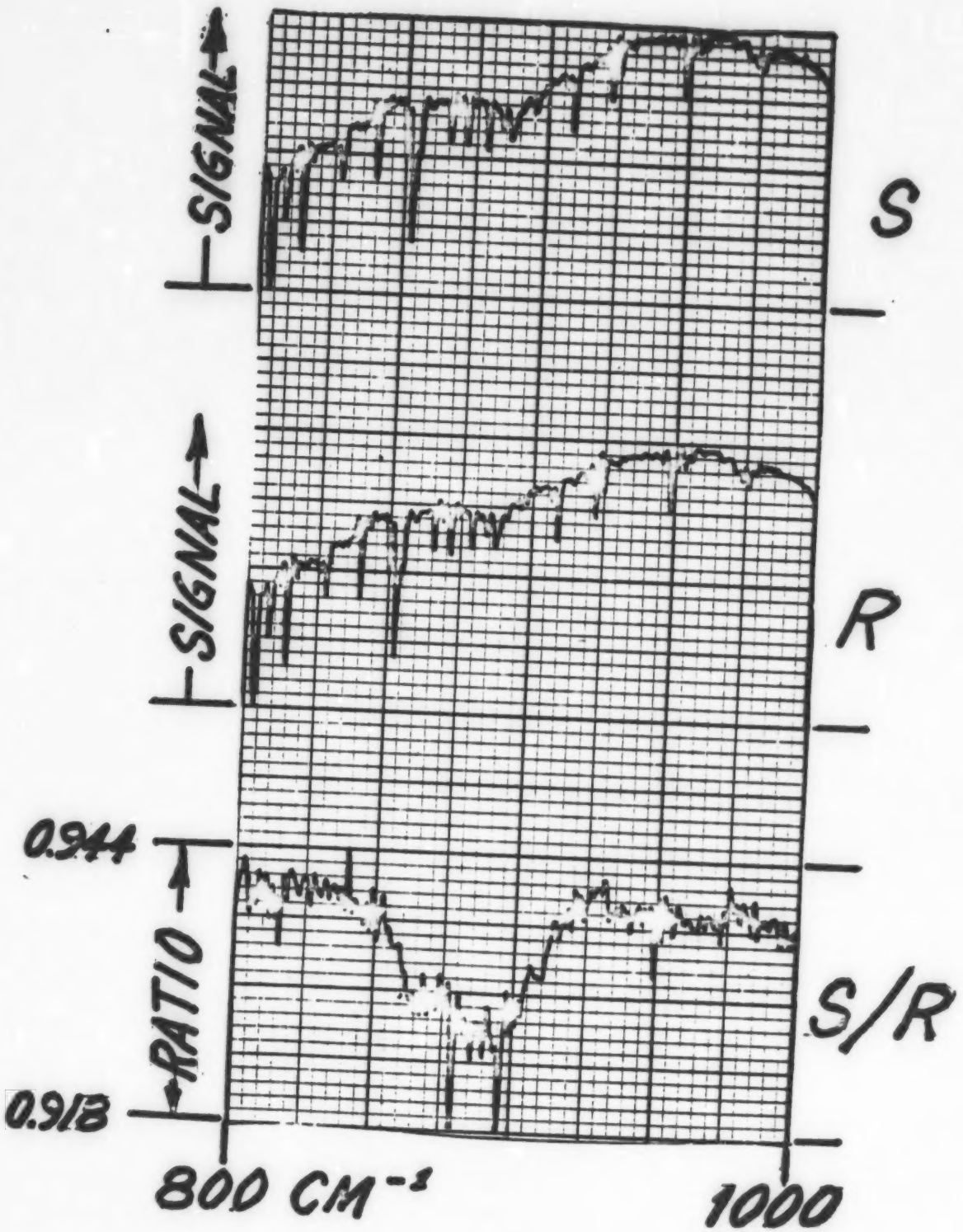
SIGNAL
S
SIGNAL
R
0.944
RATIO
0.918
S/R
800 CM⁻¹
1000

Figure 11. Measurement of 3 PPB C_2H_4 in Room Air. Path, 471 Meters; Resolution, 2 cm^{-1} With Smoothed Plotting

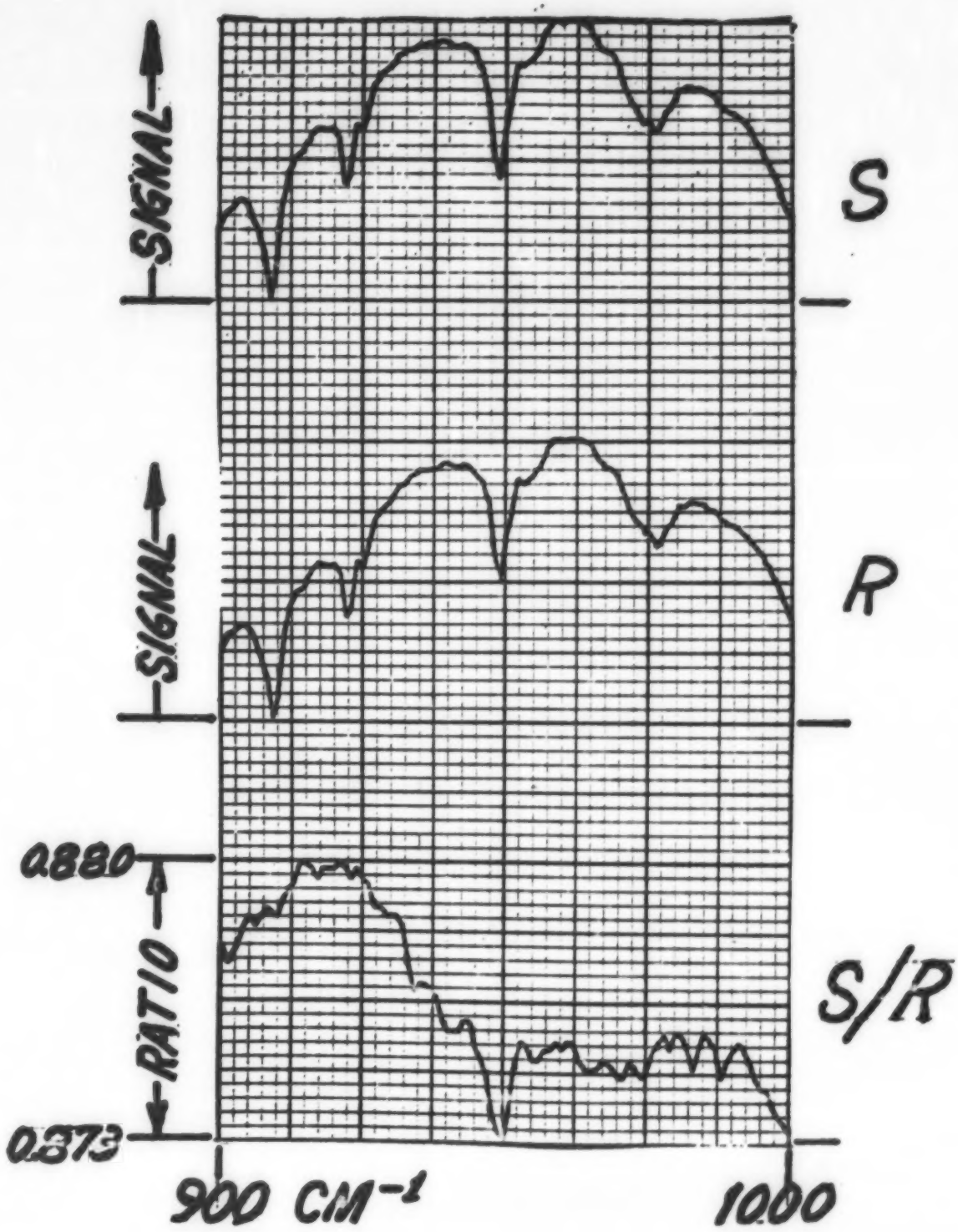
SIGNAL
S
SIGNAL
R
0.880
RATIO
0.373
S/R
900 CM-1
1000

peaks at 879 and 896 cm^{-1}. The peak at 896 cm^{-1} can just barely be seen in the single beam sample spectrum at the top of the figure.

Figure 11 shows the measurement of approximately 3 parts-per-billion of ethylene in room air with a path length of 471 meters. This is a spectrum recorded with resolution of 2 cm^{-1} but plotted with computer smoothing which gives the lines an apparent width of about 5 cm^{-1}.

VII. Detectability Limits

It can be assumed that one can detect any spectral line or band which is approximately as strong as the noise level in the spectrum. Detectability is increased in direct response to the reduction of the noise. The noise level is a function of the source intensity, the number of scans, the spectral resolution, the types of optical filters used, the stability of the optical components and other operational factors. When plotting in the ratio mode at paths of several hundred meters, a signal-to-noise level of about 2000 has been achieved, corresponding to a single-pass signal-to-noise level of roughly 10,000. Using this figure and known absorption coefficients we calculate the limits of detectability at a given path length, as follows.

The path length for maximum signal-to-noise level is a function of the mirror reflectivity. The detection limit for faint absorption will be improved by pathlength increases and degraded by reflection losses. The optimum conditions in the multiple pass cell are discussed below using the approach outlined by Stephens and by Hirschfeld.[13][14]

Assume the following definitions:

N_1 - Noise level, as a fraction of the total signal, after one pass.

P - Cell transmittance per pass.

S_1 - Absorption signal (peak depth), as a fraction of the total signal.

n - Number of passes.

N_n - Noise level, after n passes.

S_n - Absorption signal (peak depth), after n passes.

T_n - Cell transmittance for n passes relative to value for a single pass.

First we consider that the cell transmittance is the product of the transmittances per pass:

$$T_n = P^n \tag{1}$$

Therefore:

$$N_n = \frac{N_1}{T_n} = N_1 P^{-n} \tag{2}$$

and, for weak absorption peaks:

$$S_n = S_1 n \tag{3}$$

We then form the ratio:

$$\frac{S_n}{N_n} = \frac{S_1 n}{N_1} P^n \tag{4}$$

Differentiation shows that this signal-to-noise ratio is at maximum when:

$$n = \frac{1}{-\ln P} \tag{5}$$

Using equations (1), (4) and (5), we can now write:

$$(S_n/N_n)_{max} = (S_1/N_1)\, T_n/-\ln P \tag{6}$$

From equation (1)

$$\ln T_n = n \ln P \tag{7}$$

Combining equations (5) and (7) gives:

$$T_n = 1/e = 0.37 \tag{8}$$

Combining equations (6) and (8) gives:

$$\frac{(S_n/N_n)max}{(S_1/N_1)} = \frac{-0.37}{\ln P} \qquad (9)$$

Which for $P \to 1$ can be approximated as:

$$\frac{(S_n/N_n)max}{(S_1/N_1)} = \frac{0.37}{1-P} \qquad (10)$$

Let us now assume that a peak can be seen when its depth is equal to the noise amplitude ($S_n/N_n = 1$). We can then obtain the minimum detectable concentration of a gaseous compound as a function of (1) the product of the absorption coefficient and the length of a single pass, $a \cdot L$, (2) the cell transmittance per pass, P, and (3) the initial noise level, N_1. P will be slightly less than unity because of absorption and scattering losses at the mirror surfaces. For new mirrors, P can be greater than 0.99. For soiled mirrors, P may fall to 0.95. Equations (5) and (10) yield values of n that give the maximum (S_n/N_n) and values of (S_1/N_1) that make this maximum (S_n/N_n) equal to unity. Selecting a value for N_1 then yields values of S_1. The absorption equation is then used as follows:

$$S_1 = \ln I_o/I = a \cdot L \cdot c \qquad (11)$$

I_o - The incident intensity.

I - The transmitted intensity.

a - The absorption coefficient, whose values typically fall in the range 10 to 50 cm^{-1} - atm^{-1}.

L - The length of a single pass in centimeters.

c - The partial pressure of a gaseous absorber, in atmospheres.

Combining equations (10) and (11) then gives the minimum detectable concentration of a compound, $c_{min.}$, as a function of a, L, N_1, and P.

$$C_{min.} = \frac{(1 - P) \cdot N_1}{0.37 \cdot a \cdot L} \qquad (12)$$

If we assume a single-pass noise level, N_1, one ten-thousandth of the total signal, a base path, L, of 1000 centimeters, a typical absorption coefficient, a, of 30 cm^{-1} - atm^{-1}, and a mirror reflectivity, P, of 98%, we calculate that we can detect 1.8×10^{-10} atmospheres of the compound. Equation (5) also tells us that the number of passes to be used in this case is 50.

For this example we show in Table I the values of $C_{min.}$ for a number of important air pollutants. The absorption coefficients cover a wide range, but in most cases, the limit of detectability is below a part-per-billion. Generally, one can allow a factor of ten degradation of sensitivity due to interferences and other practical difficulties and still have a detection limit below the level of the ambient atmospheric pollution. In the cities the pollution levels are much higher than the limits shown in the table. For urban air monitoring, one could use an absorption cell much smaller than the 10 meter cell considered in the example.

VIII. Continuation of Work

The work is being continued in the laboratory and in the field. In the laboratory, photochemical reactions are being studied with such systems as NO_2-ethylene-air, auto exhaust-air, and NO_2-aromatics-air. Although these systems have been studied before, the extended capabilities of the new infrared system are yielding important new data on them, to be reported subsequently.

The field studies are being conducted in St. Louis, Missouri and in Pasadena, California. For use in St. Louis, a long path cell of the eight-mirror type described in reference 9 is being installed in a mobile van along with the Fourier Transform Spectrometer. This cell has a 5.2 meter base

path with a mirror reflectivity of 98% or higher. Ambient air at the van location will be taken into the cell and analyzed. Air samples at distant locations will be collected in plastic bags and brought to the van for analysis. A similar system with an 8.7 meter base path is being installed on a rooftop in Pasadena where it will provide a new highly sensitive analysis of the Southern California photochemical pollution.

TABLE I - Estimates of Pollutant Detectability Limits, Using 50 Passes Through a 10 Meter Cell, With 98% Mirror Reflectivity.

Pollutant	Best Measurement Frequency (cm^{-1})	Detectability Limit $c_{min.}$ in Billionths of an Atmosphere (PPB)	References and Remarks
Acetylene	735	0.02	Absorption coefficient measured in the present work. This is the strongest band we have seen in any spectrum.
Ammonia	965	0.2	Reference 9.
Carbon Monoxide	2180	1.0	Reference 9. The atmospheric carbon monoxide concentration never falls below about 80 PPB.
Ethylene	950	0.2	Reference 9.
Formaldehyde	2765	1.0	Reference 9. This estimate is for 1 cm^{-1} resolution. Higher resolution may further increase the detection sensitivity.
Formic Acid	1100	0.8	Reference 15.
Hydrogen Chloride	2820	1.0	Reference 9. This estimate is for 1 cm^{-1} resolution. Higher resolution may further increase the detection sensitivity.
Hydrogen Sulfide	1300	50	Reference 15. H_2S has the weakest spectrum we have seen from a polyatomic pollutant molecule.
Methane	3020	0.6	Reference 9. The atmospheric methane concentration never falls below 1400 PPB.
Nitric Acid	880	0.6	Reference 15.
Nitric Oxide	1900	2.0	Reference 9.
Nitrogen Dioxide	1615	0.2	Absorption coefficient measured in the present work.

TABLE I - Continued

Pollutant	Best Measurement Frequency (cm^{-1})	Detectability Limit $c_{min.}$ in Billionths of an Atmosphere (PPB)	References and Remarks
Ozone	1060	0.6	Reference 9.
Peroxy Acetyl Nitrate	1160	0.2	Reference 16.
Peroxy Benzoyl Nitrate	990	0.2	Reference 8.
Phosgene	850	0.1	Reference 15.
Propylene	915	1.0	Reference 9.
Sulfur Dioxide	1360	0.2	Reference 15.

REFERENCES

1. Ralph Stair, Proc. Natl. Air Pollution Symp. 3rd, Pasadena, Calif., Western Oil and Gas Association, Los Angeles, 1955.

2. David M. Gates, Proc. Natl. Air Pollution Symp. 3rd, Pasadena, Calif., Western Oil and Gas Association, Los Angeles, 1955.

3. M. Nigeotte, L. Neven, and J. Swensson, "The Solar Spectrum from 2.8 to 23.7 Microns, Part I Photometric Atlas", in Memoirs de la Societe Royale des Sciences de Liege, Special Vol. No. 1, 1956.

4. D. Murcray, T. Kyle, F. Murcray, and W.J. Williams, Presence of HNO_3 in the Upper Atmosphere, J. Opt. Soc. of America 59, 1131 (1969).

5. E.R. Stephens, P.L. Hanst, R.C. Doerr, and W.E. Scott, Reactions of Nitrogen Dioxide and Organic Compounds in Air, Ind. and Eng. Chem., 48, 1498 (1956).

6. W.E. Scott, E.R. Stephens, P.L. Hanst, and R.C. Doerr, Further Developments in the Chemistry of the Atmosphere, Proc. A.P.I., 37, (III), 171 (1957).

7. C.S. Tuesday in "Chemical Reactions in the Lower and Upper Atmosphere", R.D. Cadle, Ed.) Interscience, New York, 1961, pp 1-49.

8. J.M. Huess and W.A. Glasson, "Hydrocarbon Reactivity and Eye Irritation", Env. Sci. and Technology, 2, 1109 (1968).

9. Philip L. Hanst, Spectroscopic Methods for Air Pollution Measurement, pages 91 through 213 of Advances in Environmental Science and Technology, Volume II, J.N. Pitts and R.L. Metcalf, Editors, John Wiley and Sons, Inc., 1971.

10. R. Curbelo and C. Foskett, Paper No. 21 at the Aspen International Conference on Fourier Spectroscopy 1970, Special Report No. 114, Air Force Cambridge Research Laboratory, L.G. Hanscom Field, Bedford, Mass., January 5, 1971.

11. J.U. White, Long Optical Paths of Large Aperture, J. Opt. Soc. Amer., 32, 285 (1942).

12. C. Junge and J. Hahn, N_2O Measurements in the North Atlantic, J. of Geophysical Research 76, 8143 (1971).

13. E.R. Stephens, Applied Spectroscopy 12, 80 (1958).

14. T. Hirschfeld, FTS Notes, Digilab Co., Cambridge, Mass. (1972).

15. R.H. Pierson, A.N. Fletcher, and E. St. Clair Gantz, Catalog of Infrared Spectra for Qualitative Analysis of Gases, Analytical Chemistry 28, 1218 (1956).

16. E.R. Stephens, Absorptivities for Infrared Determination of Peroxyacyl Nitrates, Analytical Chemistry 36, 928 (1964).